Determining Cosmological Parameters with Latest Observational Data

Jun-Qing Xia[a,c], Hong Li[b,c], Gong-Bo Zhao[d], and Xinmin Zhang[a,c]
[a] *Institute of High Energy Physics, Chinese Academy of Science, P.O.Box 918-4, Beijing 100049, P.R.China*
[b] *Department of Astronomy, School of Physics, Peking University, Beijing 100871, P.R.China*
[c] *Theoretical Physics Center for Science Facilities (TPCSF), Chinese Academy of Science, P.R.China and*
[d] *Department of Physics, Simon Fraser University, Burnaby, BC V5A 1S6, Canada*

In this paper, we combine the latest observational data, including the WMAP five-year data (WMAP5), BOOMERanG, CBI, VSA, ACBAR, as well as the Baryon Acoustic Oscillations (BAO) and Type Ia Supernoave (SN) "Union" compilation (307 sample), and use the Markov Chain Monte Carlo method to determine the cosmological parameters, such as the equation-of-state (EoS) of dark energy, the curvature of universe, the total neutrino mass and the parameters associated with the power spectrum of primordial fluctuations. Our results show that the ΛCDM model remains a good fit to the current data. In a flat universe, we obtain the tight limit on the constant EoS of dark energy as, $w = -0.977 \pm 0.056$ ($1\ \sigma$). For the dynamical dark energy models with time evolving EoS parameterized as $w_{\rm de}(a) = w_0 + w_1(1-a)$, we find that the best-fit values are $w_0 = -1.08$ and $w_1 = 0.368$, implying the preference of Quintom model whose EoS gets across the cosmological constant boundary during evolution. For the curvature of universe Ω_k, our results give $-0.012 < \Omega_k < 0.009$ (95% C.L.) when fixing $w_{\rm de} = -1$. When considering the dynamics of dark energy, the flat universe is still a good fit to the current data, $-0.015 < \Omega_k < 0.018$ (95% C.L.). Regarding the neutrino mass limit, we obtain the upper limits, $\sum m_\nu < 0.533$ eV (95% C.L.) within the framework of the flat ΛCDM model. When adding the SDSS Lyman-α forest power spectrum data, the constraint on $\sum m_\nu$ can be significantly improved, $\sum m_\nu < 0.161$ eV (95% C.L.). However, these limits can be weakened by a factor of 2 in the framework of dynamical dark energy models, due to the obvious degeneracy between neutrino mass and the EoS of dark energy model. Assuming that the primordial fluctuations are adiabatic with a power law spectrum, within the ΛCDM model, we find that the upper limit on the ratio of the tensor to scalar is $r < 0.200$ (95% C.L.) and the inflationary models with the slope $n_s \geq 1$ are excluded at more than $2\ \sigma$ confidence level. However, in the framework of dynamical dark energy models, the allowed region in the parameter space of (n_s,r) is enlarged significantly. Finally, we find no strong evidence for the large running of the spectral index, $\alpha_s = -0.019 \pm 0.017$ ($1\ \sigma$) for the ΛCDM model and $\alpha_s = -0.023 \pm 0.019$ ($1\ \sigma$) for the dynamical dark energy model, respectively.

I. INTRODUCTION

With the accumulation of observational data from cosmic microwave background measurements (CMB), large scale structure surveys (LSS) and supernovae observations and the improvements of the data quality, the cosmological observations play a crucial role in our understanding of the universe, and also in constraining the cosmological parameters, such as the EoS of dark energy models, the curvature of universe, the total neutrino masses and those associated with the running of the spectral index and gravitational waves. In our previous work [1], we have used the Markov Chain Monte Carlo (MCMC) method to constrain cosmological models from the astronomical observational data, including the WMAP three-year data (WMAP3) [2, 3], small-scale CMB data, LSS data [4, 5] and SNIa ESSENCE sample [6]. We found that the cosmological constant is consistent with the data, however the dynamical dark energy models are still allowed and interestingly the model with its EoS getting across $w = -1$ the *Quintom* model [7] is the best fit model. And we found no strong significant evidence for the non-flat universe and massive neutrino. Within the ΛCDM model, the scale-invariant spectrum and the spectra with $n_s > 1$ are disfavored by more than $2\ \sigma$ confidence level. Due to the degeneracy between the EoS of dark energy and tensor fluctuation, those inflationary models excluded within the ΛCDM model, will revive in the framework of dynamical dark energy models. Furthermore, we did not find any significant evidence for the tensor fluctuations and the large running of the spectral index.

Given the precision of current observations, these results are not conclusive for the time being. Recently, the WMAP experiment has published its five-year data of temperature and polarization power spectra [8, 9, 10]. The Arcminute Cosmology Bolometer Array (ACBAR) experiment has also published its new CMB temperature power spectrum [11]. These new CMB data can strengthen the constraints on the cosmological parameters, especially for the inflationary models [8, 9, 12]. Furthermore, the Supernova Cosmology Project has made an unified analysis of the world's supernovae datasets and presented a new compilation "Union" (307 sample) [13] which includes the recent samples of SNIa from SNLS and ESSENCE Survey, as well as some older datasets, *etc.* In the literature [13, 14], this Union compilation combining with the shift parameter derived from CMB and the BAO information has been used to constrain cosmological models. However, in these studies the CMB information considered is just the shift parameter instead of the full CMB data, which will lose some information

of CMB and lead to a biased result [15]. Thus, in this paper, we revisit the issue on the determination of these cosmological parameters and update our previous results with the latest observational data.

Our paper is organized as follows: In Section II we describe the method and the latest observational datasets we used; Section III contains our main global fitting results on the cosmological parameters and the last section is the summary.

II. METHOD AND DATA

In our study, we perform a global analysis using the publicly available MCMC package CosmoMC[1] [16]. We assume the purely adiabatic initial conditions. Our most general parameter space is:

$$\mathbf{P} \equiv (\omega_b, \omega_c, \Omega_k, \Theta_s, \tau, w_0, w_1, f_\nu, n_s, A_s, \alpha_s, r) \ , \quad (1)$$

where $\omega_b \equiv \Omega_b h^2$ and $\omega_c \equiv \Omega_c h^2$, in which Ω_b and Ω_c are the physical baryon and cold dark matter densities relative to the critical density, Ω_k is the spatial curvature and satisfies $\Omega_k + \Omega_m + \Omega_{\rm de} = 1$, Θ_s is the ratio (multiplied by 100) of the sound horizon to the angular diameter distance at decoupling, τ is the optical depth to re-ionization, f_ν is the dark matter neutrino fraction at present, namely,

$$f_\nu \equiv \frac{\rho_\nu}{\rho_{\rm dm}} = \frac{\Sigma m_\nu}{93.105 \text{ eV } \Omega_c h^2} \ . \quad (2)$$

The primordial scalar power spectrum $\mathcal{P}_\chi(k)$ is parameterized as [17]:

$$\ln \mathcal{P}_\chi(k) = \ln A_s(k_{s0}) \ + \ (n_s(k_{s0}) - 1) \ln\left(\frac{k}{k_{s0}}\right) + \ \frac{\alpha_s}{2}\left(\ln\left(\frac{k}{k_{s0}}\right)\right)^2 \ , \quad (3)$$

where A_s is defined as the amplitude of initial power spectrum, n_s measures the spectral index, α_s is the running of the scalar spectral index and r is the tensor to scalar ratio of the primordial spectrum. For the pivot scale we set $k_{s0} = 0.05{\rm Mpc}^{-1}$. Moreover, w_0 and w_1 are the parameters of dark energy EoS, which is given by [18]:

$$w_{\rm de}(a) = w_0 + w_1(1-a) \ , \quad (4)$$

where $a = 1/(1+z)$ is the scale factor and $w_1 = -dw/da$ characterizes the "running" of EoS (RunW henceforth). The ΛCDM model has $w_0 = -1$ and $w_1 = 0$. For the dark energy model with a constant EoS, $w_1 = 0$ (WCDM henceforth). When using the global fitting strategy to constrain the cosmological parameters, it is crucial to include dark energy perturbations [2, 19, 20]. In this paper we use the method provided in Refs.[20, 21] to treat the dark energy perturbations consistently in the whole parameter space in the numerical calculations.

In the computation of CMB we have included the WMAP5 temperature and polarization power spectra with the routine for computing the likelihood supplied by the WMAP team[2]. We also include some small-scale CMB measurements, such as BOOMERanG [22], CBI [23], VSA [24] and the newly released ACBAR data [11]. Besides the CMB information, we also combine the distance measurements from BAO and SNIa. For the BAO information, we use the gaussian priors on the distance ratios, $r_s/D_v(z) = 0.1980 \pm 0.0058$ at $z = 0.2$ and $r_s/D_v(z) = 0.1094 \pm 0.0033$ at $z = 0.35$, with a correlation coefficient of 0.39, measured from the BAO in the distribution of galaxies [25]. In the calculation of the likelihood from SNIa we have marginalized over the nuisance parameter [26]. The supernova data we use are the recently released "Union" compilation (307 sample) [13]. In order to improve the constraint on the total neutrino mass, we include the Lyman-α forest power spectrum from Sloan Digital Sky Survey (SDSS) [27], however also keep its unclear systematics in mind [8, 28]. Furthermore, we make use of the Hubble Space Telescope (HST) measurement of the Hubble parameter $H_0 \equiv 100$h km s^{-1} Mpc^{-1} by a Gaussian likelihood function centered around $h = 0.72$ and with a standard deviation $\sigma = 0.08$ [29].

III. NUMERICAL RESULTS

In this section we present our global fitting results of the cosmological parameters determined from the latest observational data and focus on the dark energy parameters, curvature of universe, neutrino mass and the inflationary parameters, respectively.

A. Equation of State of Dark Energy

In Table I we list the constraints on the dark energy parameters as well as the Hubble constant in different dark energy models.

Assuming the flat universe, firstly we explore the constraints on the constant EoS of dark energy, w ($w \equiv w_0$, $w_1 \equiv 0$), from the latest observational data. In Fig.1 we show the constraints on w and the present dark matter density, Ω_m. This result shows that the combination of Union compilation (with systematic uncertainties not included) and other observational data yield a

[1] Available at: http://cosmologist.info/cosmomc/.

[2] Available at the LAMBDA website: http://lambda.gsfc.nasa.gov/.

TABLE I. Constraints on the dark energy EoS and some background parameters from the latest observations. Here we have shown the mean and the best fit values, which are obtained from the cases with and without the systematic uncertainties of Union compilation, respectively.

Parameter		w_0		w_1		$\Omega_{\rm de}$		H_0	
		with sys	w/o sys	with sys	w/o sys	with sys	w/o sys	with sys	w/o sys
ΛCDM	BestFit	-1	-1	0	0	0.735	0.741	71.0	71.6
$\Omega_k = 0$	Mean	-1	-1	0	0	0.738 ± 0.015	0.738 ± 0.014	71.4 ± 1.4	71.4 ± 1.3
WCDM	BestFit	-0.978	-0.955	0	0	0.738	0.735	71.4	70.6
$\Omega_k = 0$	Mean	-0.965 ± 0.080	-0.977 ± 0.056	0	0	0.736 ± 0.016	0.737 ± 0.014	70.8 ± 1.9	71.1 ± 1.4
RunW	BestFit	-1.09	-1.08	0.533	0.368	0.735	0.738	70.4	71.1
$\Omega_k = 0$	Mean	-0.946 ± 0.194	-0.993 ± 0.128	-0.133 ± 0.749	0.030 ± 0.582	0.734 ± 0.017	0.737 ± 0.014	70.7 ± 1.9	70.9 ± 1.5
RunW	BestFit	–	-1.11	–	0.475	–	0.739	–	72.4
$\Omega_k \neq 0$	Mean	–	-0.976 ± 0.148	–	-0.071 ± 0.848	–	0.736 ± 0.014	–	70.9 ± 1.9
RunW	BestFit	–	-1.04	–	0.290	–	0.742	–	71.3
w/o Pert.	Mean	–	-1.00 ± 0.114	–	0.103 ± 0.413	–	0.736 ± 0.012	–	70.8 ± 1.5

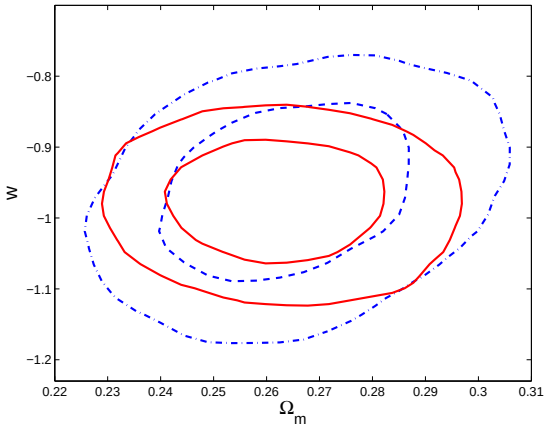

FIG. 1: Constraints on the constant EoS of dark energy, w, and the present matter density, Ω_m, from the latest observations, assuming a flat universe. The blue dash-dot lines and red solid lines are obtained with and without the systematic uncertainties of Union compilation, respectively.

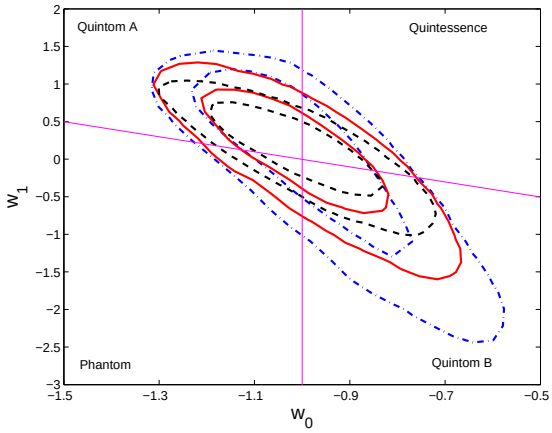

FIG. 2: Constraints on the dark energy EoS parameters w_0 and w_1 from the current observations, CMB+BAO+SN. The red solid lines and the blue dash-dot lines are obtained for the flat and non-flat universe, respectively. And the black dashed lines are obtained when (incorrectly) neglecting dark energy perturbations. The magenta solid lines stand for $w_0 = -1$ and $w_0 + w_1 = -1$. In this numerical calculation the systematic uncertainties of Union compilation is not considered.

strong constraint on the constant EoS of dark energy, $w = -0.977 \pm 0.056$ ($1\ \sigma$). Our result is similar to the limit from WMAP5 [8], $w = -0.972^{+0.061}_{-0.060}$ ($1\ \sigma$) and physically it indicates that $w = -1$ is consistent with the data. Furthermore, some of the quintessence models get strongly constrained, for example, the tracker quintessence model which predicts $w \sim -0.7$ [30] will be excluded by more than 5 σ. However we notice that the systematic uncertainties of Union compilation will affect strongly the error estimation of dark energy parameters [13]. If taking the systematic uncertainties into account, we find the limit on the constant EoS of dark energy is $w = -0.965 \pm 0.080$ ($1\ \sigma$) and the error bar is significantly enlarged.

For the time evolving EoS, $w_{\rm de}(a) = w_0 + w_1(1-a)$, in Fig.2 we illustrate the constraints on the dark energy parameters w_0 and w_1. For the flat universe, from the latest observational data we find that the best fit model is the Quintom dark energy model, $w_0 = -1.08$ and $w_1 = 0.368$, whose $w(z)$ can cross the cosmological constant boundary during the evolution. But then the variance of w_0 and w_1 are still large, namely, the 95% constraints on w_0 and w_1 are $-1.22 < w_0 < -0.721$ and $-1.33 < w_1 < 0.947$. This result implies that the dynamical dark energy models are not excluded and the current data cannot distinguish different dark energy models decisively. The ΛCDM model, however is still a good fit right now.

Our results are consistent with the WMAP5 group [8], while the upper limit on w_0 and lower limit on w_1 are slightly weaker than theirs. This difference is mainly from the supernovae datasets used. The supernovae dataset we use in this paper is the new Union compilation with homogeneous analysis of the present world's super-

novae data. But in Ref.[8] they use three supernovae datasets, SNLS [31], HST [32] and ESSENCE [6]. For each of them, they marginalize over the absolute magnitude separately, and simply add these three pieces to get the total χ^2.

Because the parametrization of EoS of the dark energy used in this paper is assumed to extend to an arbitrary high redshift, it is important to check if the energy density of dark energy component is negligible compared with the radiation density at the epoch of the Big Bang Nucleosynthesis (BBN), $z \sim 10^9$. As shown by the red solid lines in Fig.2, the dynamical dark energy models allowed by the current data within the 95% confidence level safely satisfy the limits of $w_0 + w_1 < 0$ and BBN [33, 34] to avoid the dark energy domination in the early universe.

Furthermore, the Null Energy Condition (NEC) should also be satisfied for the EoS of universe w_u [35]:

$$w_u(a) \equiv \frac{\sum w_i(a)\rho_i(a)}{\sum \rho_i(a)} \geq -1 \ , \qquad (5)$$

where w_i and ρ_i are the EoS and energy density for component i in the universe. Violation of NEC will lead to the breakdown of causality in general relativity and the violation of the second law of thermodynamics [36]. This requirement from $w_u(a) \geq -1$ will constrain the EoS parameters of dark energy models [37].

Firstly, we consider the WCDM dark energy model. From Table I, the current observational data give the present energy density of dark energy $\Omega_{\rm de} \simeq 0.74$. If we just assume that the EoS of dark energy is constant from the early time of universe to present, using the above Eq.(5), we obtain that the NEC limit requires the EoS of dark energy $w_{\rm de} \gtrsim -1.35$ straightforwardly [38]. Fortunately, the current constraints on $w_{\rm de}$ with and without the systematic uncertainties of "Union" compilation satisfy this limit safely. However, if we extend the period of validity of constant EoS of dark energy into the future where the dark energy component will dominate the universe entirely (namely $\Omega_{\rm de} \approx 1$), the NEC requires $w_{\rm de} \gtrsim -1$. Consequently, the phantom dark energy models ($w_{\rm de} < -1$) will be excluded and the fate of universe with Big Rip [39] could not happen.

For the RunW dark energy model, we illustrate the constraints on the dark energy parameters w_0 and w_1 from the current observations (black solid lines) and the NEC (blue dashed lines) in Fig.3, respectively. In the upper panel, the parameterized EoS $w_{\rm de} = w_0 + w_1(1-a)$ is assumed to be valid until now, not for the future, *i.e.* $0 \leq a \leq 1$. The reasons for doing this are i) experimentally there are no constraints on the dark energy models for the future universe; ii) theoretically it is always possible to choose a different type of parametrization of dark energy EoS for the future universe, such as $w_{\rm de} = w_0 \exp(1-a)$ for $a > 1$, which matches to $w_{\rm de} = w_0 + w_1(1-a)$ at $a = 1$ and satisfies the NEC [37]. In fact, if the current EoS of dark energy $w_0 < -1$, this scenario allows the transition from $w_{\rm de} < -1$ to $w_{\rm de} > -1$, consequently avoids the violation of NEC. One can see from the Fig.3, in this case, the NEC limit does improve the constraints on dark energy parameters from the current observations. For example, the current observational data permit $w_0 < -1.35$ at 2 σ confidence level, which however violates the NEC limit.

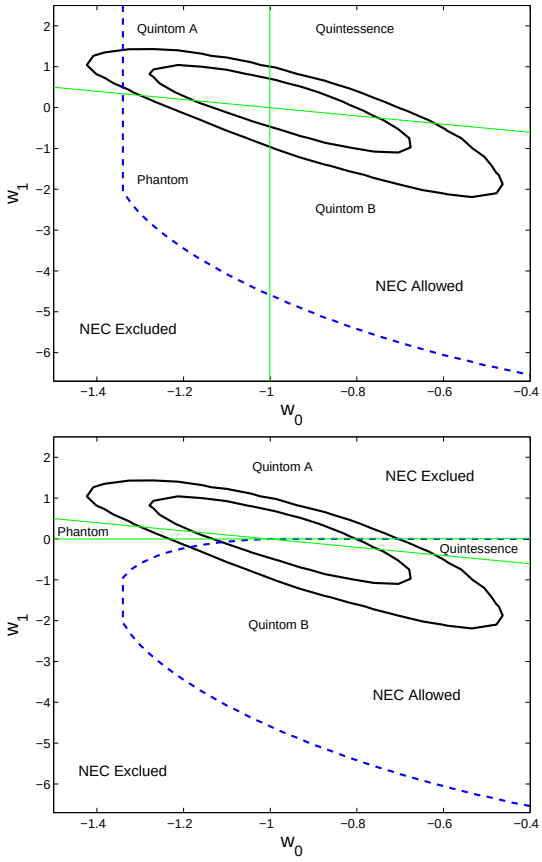

FIG. 3: Constraints on the dark energy EoS parameters w_0 and w_1 from the current observations (black solid lines) and the Null Energy Condition (blue dashed lines). In the upper panel, the parametrization of EoS in Eq.(4) is assumed to be a description of dark energy for the past until now. In the lower panel, we assume that the parametrized EoS are also valid for the far future.

In the lower panel of Fig.3, the parametrization $w_{\rm de} = w_0 + w_1(1-a)$ is assumed to be a valid description of dark energy model at any time from the far past to the far future. One can see from this figure, the NEC puts a stronger constraint on the EoS parameters of dark energy models than the observational data. For this case, the regions of quintessence and phantom dark energy models will be shrunk significantly in the (w_0,w_1) space, and the NEC excludes the dark energy models corresponding to the regions labelled by the phantom and Quintom A with $w_{\rm de} < -1$ for $a \to \infty$. Consequently, the models satisfying the NEC include the quintessence and some of the Quintom B dark energy models, which can be seen in the lower panel of Fig.3.

TABLE II. Constraints on cosmological parameters n_s, α_s, r, Ω_k and $\sum m_\nu$ from the current observations. We have shown the mean $1,2\ \sigma$ errors. For the weakly constrained parameters we quote the 95% upper limits instead.

Parameters	ΛCDM	RunW
$100\times\Omega_k$	$-0.081^{+0.545+1.025}_{-0.524-1.161}$	$0.098^{+0.881+1.655}_{-0.881-1.605}$
$\sum m_\nu$	<0.533 (95%)	<0.974 (95%)
$\sum m_\nu$ (w/ Lyα)	<0.161 (95%)	<0.252 (95%)
n_s	$0.961^{+0.012+0.024}_{-0.012-0.023}$	$0.964^{+0.013+0.027}_{-0.013-0.025}$
α_s	$-0.019^{+0.017+0.032}_{-0.017-0.030}$	$-0.023^{+0.019+0.039}_{-0.019-0.037}$
r	<0.200 (95%)	<0.268 (95%)

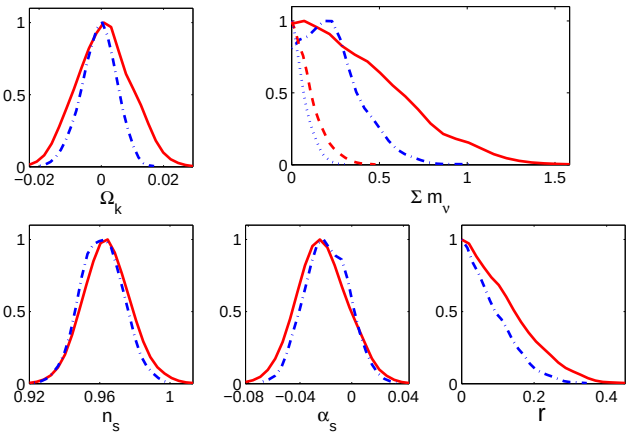

FIG. 4: $1D$ current constraints on the inflationary parameters n_s, α_s and r, as well as the curvature Ω_k and the total neutrino mass $\sum m_\nu$, in different dark energy models: ΛCDM model (blue dash-dot lines) and RunW model (red solid lines). For $\sum m_\nu$, we also show the limits combined with the SDSS Lyman-α forest power spectrum. Blue dotted lines and red dashed lines denote the ΛCDM and RunW models, respectively.

Finally we discuss the degeneracy between the dark energy and curvature. As we know, the EoS of dark energy is degenerated with the curvature of universe Ω_k [40, 41]. If we do not include the prior that the universe is flat, from Table I and the blue dash-dot lines in Fig.2, we can see that the constraints on w_0 and w_1 are weakened significantly and the two-dimensional distribution extends more towards the Quintom B region. But the main conclusions are unchanged, $w_0=-1.11$ and $w_1=0.475$, namely, the Quintom dark energy model is still mildly favored by the current observational data. Moreover, in order to show the importance of dark energy perturbations in the global analysis, we do the calculation by incorrectly neglecting the dark energy perturbations. Illustrated as the black dashed lines in Fig.2, one can see that the constraints on the dark energy parameters become tighter immediately, similar to our previous results [20]. This study shows that how biased the result will be, once the dark energy perturbations are incorrectly neglected in the analysis [2, 15, 20].

B. Curvature of Universe

The measurements on the position of first acoustic peak of CMB temperature power spectrum have been used to determine the curvature of universe Ω_k. However, due to the well-known degeneracy between Ω_m and Ω_k, we have to add other cosmological data, such as the large scale structure and supernovae data, to break this degeneracy and improve the constraint. Within the ΛCDM model, from Table II and Fig.4, we can see that our universe is very close to flatness, namely, the 95% limit is $-0.012<\Omega_k<0.009$, which is consistent with the prediction of inflation paradigm.

As we mentioned before, dark energy parameters and Ω_k are correlated via the cosmological distance information. In the framework of dynamical dark energy models, the constraint on Ω_k should be relaxed. Based on the calculations, we can see that the combination of observational data implies $-0.015<\Omega_k<0.018$ at $2\ \sigma$ confidence level.

C. Neutrino Mass

Detecting the neutrino mass is one of the challenges of modern physics. Currently the neutrino oscillation experiments, such as atmospheric neutrinos experiments [42] and solar neutrinos experiments [43], have confirmed that the neutrinos are massive, but give no hint on their absolute mass scale. Fortunately, cosmological observational data can provide the crucial complementary information on absolute neutrino masses, because massive neutrinos leave imprints on the cosmological observations, such as the Hubble diagram, CMB temperature power spectrum and LSS matter power spectrum [44].

Within the ΛCDM model, from Table II one can read 95% upper limit of the total neutrino mass derived from the current observations, CMB+LSS+SN, $\sum m_\nu<0.533$ eV (95% C.L.), which is consistent with the recent results from WMAP5 group [8, 9]. However, there are degeneracies between the neutrino mass and other cosmological parameters, such as the EoS parameters of dark energy [45] and the running of spectral index [46]. Due to the degeneracy among dark energy parameters and the neutrino mass [2, 45, 47], in the framework of dynamical dark energy models, the limit on the neutrino mass can be relaxed to $\sum m_\nu<0.974$ eV (95% C.L.) significantly, as shown in Fig.4.

It is well known that when neutrinos become non-relativistic at late time of the universe, they damp the perturbations within their free streaming scale. Thus the massive neutrinos will suppress the matter power spectrum at small scale by roughly $\Delta P/P\sim-8\Omega_\nu/\Omega_m$ [48]. Therefore, Lyman-α forest data at small scale can significantly improve the constraint on the neutrino mass.

But when we use the Lyα data, we should keep in mind on their unclear systematics right now [8, 28]. When including the SDSS Lyα forest power spectrum [27], we can obtain a much more stringent 2 σ upper limit $\sum m_\nu < 0.161$ eV in the ΛCDM model.

Moreover, the Heidelberg-Moscow (HM) experiment, which is controversial for the time being, uses the half-life of $0\nu2\beta$ decay to constrain the effective Majorana mass and this translates to the constraint on the sum of neutrino masses under some assumptions [49], $\sum m_\nu \sim 1.8 \pm 0.6$ eV (95% C.L.). We can find an obvious tension on the neutrino mass limits from between the cosmological observations and the HM experiment, which however can be resolved if the neutrino masses vary during the evolution of the universe [50]. In order to be consistent with the observational data, the neutrino mass must be very small in the past, but has grown recently in order to agree with the HM experiment data.

Again, in the RunW model, the limit on the neutrino mass is relaxed, $\sum m_\nu < 0.252$ eV (95% C.L.), which implies the existence of degeneracy between the dark energy parameters and neutrino mass.

D. Inflationary Parameters

Inflation, the most attractive paradigm in the very early universe, has successfully resolved many problems existing in hot Big Bang cosmology, such as flatness, horizon, monopole problem and so forth [51]. Its quantum fluctuations turn out to be the primordial density fluctuations which seed the observed large scale structures and the anisotropies of CMB. Inflation theory has successfully passed several non-trivial tests. Currently, the cosmological observational data are in good agreement with a gaussian, adiabatic and scale-invariant primordial spectrum, which is consistent with single field slow-roll inflation predictions.

Within the ΛCDM model, from Fig.4, we obtain the limit on the spectral index of $n_s = 0.961 \pm 0.012$ (1 σ), which excludes the scale-invariant spectrum, $n_s = 1$, and the spectra with blue tilt, $n_s > 1$, at more than 3 σ confidence level. When considering the gravitational waves, the latest observational data yield the 95% upper limit of tensor-to-scalar ratio $r < 0.200$. In Fig.5 we show the two dimensional constraints in (n_s,r) panel which can be compared with the prediction of the inflation models. We find that the Harrison-Zel'dovich-Peebles scale-invariant (HZ) spectrum ($n_s = 1$, $r = 0$) is still disfavored more than 2 σ confidence level. And many hybrid inflation models and the inflation models with "blue" tilt ($n_s > 1$) are also excluded by the current observations. Furthermore, the single slow-rolling scalar field with potential $V(\phi) \sim m^2\phi^2$, which predicts $(n_s, r) = (1 - 2/N, 8/N)$, is still well within 2 σ region, while another single slow-rolling scalar field with potential $V(\phi) \sim \lambda\phi^4$, which predicts $(n_s, r) = (1 - 3/N, 16/N)$, has been excluded more than 2 σ [8, 12, 52].

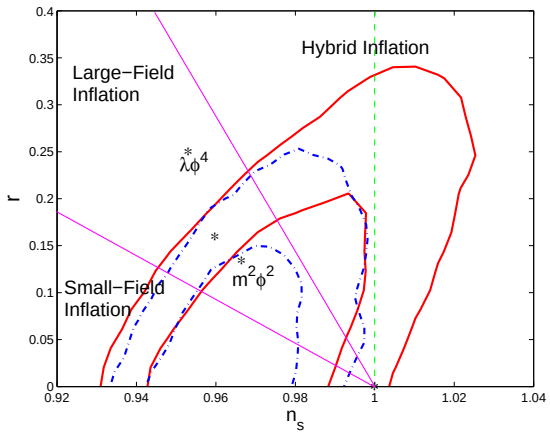

FIG. 5: 68% and 95% constraints on the panel (n_s,r) based on the different Dark Energy models: ΛCDM model (blue dash-dot lines) and RunW model (red solid line). The two magenta solid lines delimit the three classes of inflationary models, namely, small-field, large-field and hybrid models. The star points are predicted by HZ spectrum, $m^2\phi^2$ model and $\lambda\phi^4$ model, respectively. These predictions assume that the number of e-foldings, N, is $50-60$ for $m^2\phi^2$ model and 64 for $\lambda\phi^4$ model.

However, the tensor fluctuations and the dark energy component, through the ISW effect, are correlated, which mostly affect the large scale (low multipoles) temperature power spectrum of CMB [1, 53]. In the framework of dynamical dark energy model, we find that the upper limit of r can be relaxed to $r < 0.268$ (95% C.L.). Furthermore, the 95% confidence level contour in (n_s,r) panel will be enlarged consequently and the distribution extends towards the hybrid inflation region. Therefore, we can see that the HZ spectrum is consistent with the latest observational data and many hybrid inflationary models, the inflationary models with "blue" tilt ($n_s > 1$), which are excluded in the ΛCDM model, have revived in the framework of dynamical dark energy model as illustrated in Fig.5.

Finally, we explore the constraint on the running of the spectral index from the latest observational data. When combining the WMAP1 or WMAP3 data with other astronomical data, the previous analysis have found a significant evidence for large running [54, 55]. Physically this large running would be a great challenge to the single-field inflation models [56, 57]. The combination of the current observational data yield the limit on the running of the spectral index of $\alpha_s = -0.019 \pm 0.017$ (1 σ) for the ΛCDM model and $\alpha_s = -0.023 \pm 0.019$ (1 σ) for the RunW model, respectively. The error is dramatically reduced compared with the previous results [1, 53], beneficial from the more accurate observational data. Given the current data, we find no significant evidence for the large running of the spectral index.

IV. SUMMARY

Recently many experimental groups have published their new observational data, such as temperature and polarization power spectra of WMAP5 [8, 9, 10], temperature power spectrum of ACBAR [11] and supernovae dataset of Union compilation [13]. In this paper we report the updated constraints on the cosmological parameters from these latest observational data, such as the EoS of dark energy, curvature of universe, neutrino mass and inflation parameters.

For dark energy, we explore the constraints on two kinds of dynamical models. Assuming a flat universe, within the WCDM model, we find that the latest observational data yield the limit on the constant EoS of dark energy, $w = -0.977 \pm 0.056$ ($1\ \sigma$). For RunW model with a flat universe, we find that the best fit model is $w_0 = -1.08$ and $w_1 = 0.368$ described by the Quintom theory with EoS across the cosmological constant boundary. And because the precision of current observations are not good enough to determine the dark energy EoS conclusively, the dynamical dark energy models are not excluded and the ΛCDM model remains a good fit.

The Quintom scenario, with the particular feature that its EoS can cross the cosmological constant boundary smoothly, has been applied to many aspects of cosmology theoretically. Firstly, the Quintom dark energy models can also give rise to interesting prediction on the fates of the universe, different from the Quintessence or Phantom models, such as the cyclic universe [58, 59], an expanding universe with oscillating EoS. Secondly, applying a Quintom matter for the early universe can provide a scenario of bouncing cosmology, which can avoid the notorious issue of initial singularity [60].

Our results also show that the universe is very close to flatness and the upper limit on the total neutrino mass is $\sum m_\nu < 0.533$ eV (95% C.L.), from the combination of CMB, BAO and SN data. Given the efficiency of Lyα forest data on constraining the total neutrino mass, we also perform a calculation with the inclusion of the SDSS Lyman-α forest power spectrum and find that $\sum m_\nu < 0.161$ eV (95% C.L.). This result might lead to the exclusion of degenerate pattern of neutrino mass, when combining the results of neutrino oscillation experiments. Due to the degeneracy between the neutrino mass and EoS of dark energy, however in the presence of dynamics of dark energy, the constraints on $\sum m_\nu$ can be relaxed by a factor of 2.

Finally, for the inflationary models, within the ΛCDM framework, we find that the latest observational data prefer the inflation models with "red" tilt, namely, $n_s = 0.961 \pm 0.012$ ($1\ \sigma$) and small tensor fluctuations, $r < 0.200$ (95% C.L.). Because of the degeneracy between r and EoS of dark energy, the upper limit on r is relaxed to $r < 0.268$ (95% C.L.) and the parameter space in (n_s,r) panel are enlarged in the framework of dynamical dark energy models. Therefore, the inflationary model with HZ primordial spectrum ($n_s = 1$, $r = 0$), some hybrid models and some models with a "blue" tilt ($n_s > 1$), which are excluded more than $2\ \sigma$ confidence level in the ΛCDM model, will be consistent with the current observations now. Furthermore, in our analysis we do not find any significant evidence for the running of spectrum index.

Acknowledgements

We acknowledge the use of the Legacy Archive for Microwave Background Data Analysis (LAMBDA). Support for LAMBDA is provided by the NASA Office of Space Science. We have performed our numerical analysis on the Shanghai Supercomputer Center (SSC). We thank Yi-Fu Cai, Jie Liu and Tao-Tao Qiu for helpful discussions. This work is supported in part by National Science Foundation of China under Grant No. 10533010 and 10675136, and the 973 program No.2007CB815401, and by the Chinese Academy of Science under Grant No. KJCX3-SYW-N2. HL is supported by the China Postdoctoral Science Foundation. GZ is supported by National Science and Engineering Research Council of Canada (NSERC).

[1] J. Q. Xia, H. Li, G. B. Zhao and X. Zhang, arXiv:0708.1111.
[2] D. Spergel, *et al.*, Astrophys. J. Suppl. 170, 377 (2007).
[3] L. Page, *et al.*, Astrophys. J. Suppl. 170, 335 (2007); G. Hinshaw, *et al.*, Astrophys. J. Suppl. 170, 288 (2007); N. Jarosik, *et al.*, Astrophys. J. Suppl. 170, 263 (2007).
[4] M. Tegmark, *et al.*, Astrophys. J. 606, 702 (2004); M. Tegmark, *et al.*, Phys. Rev. D 74, 123507 (2006).
[5] S. Cole, *et al.*, Mon. Not. R. Astron. Soc. 362, 505 (2005).
[6] W. M. Wood-Vasey, *et al.*, Astrophys. J. 666, 694 (2007).
[7] B. Feng, X. Wang and X. Zhang, Phys. Lett. B 607, 35 (2005).
[8] E. Komatsu, *et al.*, arXiv:0803.0547.
[9] J. Dunkley, *et al.*, arXiv:0803.0586.
[10] E. L. Wright, *et al.*, arXiv:0803.0577; M. R. Nolta, *et al.*, arXiv:0803.0593; B. Gold, *et al.*, arXiv:0803.0715; G. Hinshaw, *et al.*, arXiv:0803.0732.
[11] C. L. Reichardt, *et al.*, arXiv:0801.1491.
[12] W. H. Kinney, E. W. Kolb, A. Melchiorri and A. Riotto, arXiv:0805.2966.
[13] M. Kowalski, *et al.*, arXiv:0804.4142.
[14] D. Rubin, *et al.*, arXiv:0807.1108.
[15] H. Li, J. Q. Xia, G. B. Zhao, Z. H. Fan and X. Zhang, arXiv:0805.1118.
[16] A. Lewis and S. Bridle, Phys. Rev. D 66, 103511 (2002).
[17] A. Kosowsky and M. S. Turner, Phys. Rev. D 52, 1739 (1995); J. E. Lidsey, A. R. Liddle, E. W. Kolb, E. J. Copeland, T. Barreiro and M. Abney, Rev. Mod.

Phys. 69, 373 (1997); S. Hannestad, S. H. Hansen, F. L. Villante and A. J. S. Hamilton, Astropart. Phys. 17, 375 (2002); S. L. Bridle, A. M. Lewis, J. Weller and G. Efstathiou, Mon. Not. R. Astron. Soc. 342, L72 (2003); B. Feng, X. Gong and X. Wang, Mod. Phys. Lett. A 19, 2377 (2004).
[18] M. Chevallier and D. Polarski, Int. J. Mod. Phys. D 10, 213 (2001).
[19] J. Weller and A. Lewis, Mon. Not. R. Astron. Soc. 346, 987 (2003).
[20] J. Q. Xia, G. B. Zhao, B. Feng, H. Li, X. Zhang, Phys. Rev. D 73, 063521 (2006).
[21] G. B. Zhao, J. Q. Xia, M. Li, B. Feng, X. Zhang, Phys. Rev. D 72, 123515 (2005).
[22] C. J. MacTavish, *et al.*, Astrophys. J. 647, 799 (2006).
[23] A. C. S. Readhead, *et al.*, Astrophys. J. 609, 498 (2004).
[24] C. Dickinson, *et al.*, Mon. Not. Roy. Astron. Soc. 353, 732 (2004).
[25] W. J. Percival, *et al.*, Mon. Not. Roy. Astron. Soc. 381, 1053 (2007).
[26] E. Di Pietro and J. F. Claeskens, Mon. Not. Roy. Astron. Soc. 341, 1299 (2003).
[27] P. McDonald, *et al.*, Astrophys. J. Suppl. 163, 80 (2006); P. McDonald, *et al.*, Astrophys. J. 635, 761 (2005).
[28] G. L. Fogli, *et al.*, arXiv:0805.2517.
[29] W. L. Freedman, *et al.*, Astrophys. J. 553, 47 (2001).
[30] P. J. Steinhardt, L. M. Wang and I. Zlatev, Phys. Rev. D 59, 123504 (1999).
[31] P. Astier, *et al.*, Astron. Astrophys. 447, 31 (2006).
[32] A. G. Riess, *et al.*, Astrophys. J. 607, 665 (2004); A. G. Riess, *et al.*, Astrophys. J. 659, 98 (2007).
[33] G. Steigman, Ann. Rev. Nucl. Part. Sci. 57, 463 (2007).
[34] E. L. Wright, Astrophys. J. 664, 633 (2007).
[35] S. W. Hawking and G. F. R. Ellis, *Cambridge University Press, Cambridge*, 1973.
[36] N. Arkani-Hamed, S. Dubovsky, A. Nicolis, E. Trincherini and G. Villadoro, JHEP 0705, 055 (2007).
[37] T. Qiu, Y. F. Cai and X. Zhang, arXiv:0710.0115.
[38] P. Creminelli, M. A. Luty, A. Nicolis and L. Senatore, JHEP 0612, 080 (2006).
[39] R. R. Caldwell, M. Kamionkowski and N. N. Weinberg, Phys. Rev. Lett. 91, 071301 (2003).
[40] G. B. Zhao, J. Q. Xia, H. Li, C. Tao, J. M. Virey, Z. H. Zhu and X. Zhang, Phys. Lett. B 648, 8 (2007).
[41] C. Clarkson, M. Cortes and B. A. Bassett, JCAP 0708, 011 (2007).
[42] K. S. Hirata, *et al.*, Phys. Lett. B 280, 146 (1992); Y. Fukuda, *et al.*, Phys. Lett. B 335, 237 (1994); Y. Fukuda, *et al.*, Phys. Rev. Lett. 81, 1562 (1998); W. W. M. Allison, *et al.*, Phys. Lett. B 449, 137 (1999); M. Ambrosio, *et al.*, Phys. Lett. B 517, 59 (2001).
[43] B. T. Cleveland, *et al.*, Astrophys. J. 496, 505 (1998); W. Hampel, *et al.*, Phys. Lett. B 447, 127 (1999); J. N. Abdurashitov, *et al.*, Phys. Rev. C 60, 055801 (1999); S. Fukuda, *et al.*, Phys. Rev. Lett. 86, 5651 (2001); S. Fukuda, *et al.*, Phys. Rev. Lett. 86, 5656 (2001); Q. R. Ahmad, *et al.*, Phys. Rev. Lett. 89, 011301 (2002); S. N. Ahmed, *et al.*, Phys. Rev. Lett. 92, 181301 (2004).
[44] A. D. Dolgov, Phys. Rept. 370, 333 (2002); J. Lesgourgues and S. Pastor, Phys. Rept. 429, 307 (2006).
[45] S. Hannestad, Phys. Rev. Lett. 95, 221301 (2005).
[46] B. Feng, J. Q. Xia, J. Yokoyama, X. Zhang and G. B. Zhao, JCAP 0612, 011 (2006).
[47] J. Q. Xia, G. B. Zhao and X. Zhang, Phys. Rev. D 75, 103505 (2007).
[48] W. Hu, D. J. Eisenstein and M. Tegmark, Phys. Rev. Lett. 80, 5255 (1998).
[49] A. De La Macorra, A. Melchiorri, P. Serra and R. Bean, Astropart. Phys. 27, 406 (2007).
[50] G. B. Zhao, J. Q. Xia and X. Zhang, JCAP 0707,010 (2007).
[51] A. H. Guth, Phys. Rev. D 23, 347 (1981); A. Albrecht and P. J. Steinhardt, Phys. Rev. Lett. 48, 1220 (1982); A. D. Linde, Phys. Lett. B 108, 389 (1982).
[52] H. Peiris and R. Easther, arXiv:0805.2154.
[53] J. Q. Xia and X. Zhang, Phys. Lett. B 660, 287 (2008).
[54] H. Peiris, *et al.*, Astrophys. J. Suppl. 148, 213 (2003).
[55] D. Spergel, *et al.*, Astrophys. J. Suppl. 170, 377 (2007); R. Easther and H. Peiris, JCAP 0609, 010 (2006).
[56] A. Kosowsky and M. S. Turner, Phys. Rev. D 52, 1739 (1995).
[57] J. Silk and M. S. Turner, Phys. Rev. D 35, 419 (1987); D. Polarski and A. A. Starobinsky, Nucl. Phys. B 385, 623 (1992); D. H. Lyth and E. D. Stewart, Phys. Rev. D 53, 1784 (1996).
[58] B. Feng, M. Li, Y. S. Piao and X. Zhang, Phys. Lett. B 634, 101 (2006).
[59] H. H. Xiong, T. Qiu, Y. F. Cai and X. Zhang, arXiv:0711.4469; H. H. Xiong, Y. F. Cai, T. Qiu, Y. S. Piao and X. Zhang, arXiv:0805.0413.
[60] Y. F. Cai, T. Qiu, Y. S. Piao, M. Li and X. Zhang, JHEP 0710, 071 (2007); Y. F. Cai, T. Qiu, R. Brandenberger, Y. S. Piao and X. Zhang, JCAP 0803, 013 (2008); Y. F. Cai, T. Qiu, J. Q. Xia, H. Li and X. Zhang, arXiv:0808.0819.